



A miniature fuel reformer system for portable power sources



Gregor Dolanc^{a,*}, Darko Belavič^d, Marko Hrovat^b, Stanko Hočevár^c, Andrej Pohar^c, Janko Petrovčič^a, Bojan Musizza^a

^a Department of Systems and Control, Jožef Stefan Institute, Jamova 39, SI-1000 Ljubljana, Slovenia

^b Department of Electronic Ceramics, Jožef Stefan Institute, Jamova 39, SI-1000 Ljubljana, Slovenia

^c Laboratory of Catalysis and Chemical Reaction Engineering, National Institute of Chemistry, Hajdrihova 19, SI-1000 Ljubljana, Slovenia

^d HIPOT-RR d.o.o., Šentpeter 18, SI-8222 Otočec, Slovenia

H I G H L I G H T S

- A miniature fuel reformer was developed and fabricated.
- Technology level reached exceeds laboratory prototype.
- The complete system was built: reactors, a combustor, evaporators and control.
- Engineering aspects focused: miniature design, integration, process control.
- Energy efficiency and other parameters were estimated experimentally.

A R T I C L E I N F O

Article history:

Received 26 May 2014

Received in revised form

18 July 2014

Accepted 4 August 2014

Available online 12 August 2014

Keywords:

Methanol reforming

Miniaturisation

Integration

Process control

A B S T R A C T

A miniature methanol reformer system has been designed and built to technology readiness level exceeding a laboratory prototype. It is intended to feed fuel cells with electric power up to 100 W and contains a complete setup of the technological elements: catalytic reforming and PROX reactors, a combustor, evaporators, actuation and sensing elements, and a control unit. The system is engineered not only for performance and quality of the reformat, but also for its lightweight and compact design, seamless integration of elements, low internal electric consumption, and safety. In the paper, the design of the system is presented by focussing on its miniaturisation, integration, and process control.

© 2014 Elsevier B.V. All rights reserved.

1. Introduction

The combination of a miniature hydrocarbon fuel reformer and fuel cell represents a portable electric power source for various portable electric devices for civil and military use. Thanks to the high energy density of hydrocarbons, this type of power source can have a much higher density of stored energy (stored electric energy per mass) than modern batteries. An important benefit is almost instant recharging by refilling the fuel.

There are two types of fuel cell-based power sources using methanol as a fuel: direct methanol fuel cells (DMFC) and reformed methanol fuel cells (RMFC) combining a fuel reformer and a fuel cell [1]. The first type (DMFC) works with liquid methanol or

methanol water solution and has a simpler structure because methanol is fed onto the anode of fuel cell directly and therefore fuel reformer is not needed. However, the efficiency and resulting energy density are lower due to high anode and cathode overpotentials. Power sources of this kind are available on the market, e.g. Ref. [2]. Polymer electrolyte membrane fuel cells (PEMFC) are usually used in DMFC power supplies. Solid oxide fuel cells (SOFC) are also very appropriate for direct methanol operation, however, they operate at a relatively high temperature (600–1000 °C) and have a long start-up time, which limits their use in miniature and portable (especially man-wearable) systems for civil or military applications. In any case, they have been adopted well in large-scale power generation systems [1]. The second type of power source (RMFC) is a combination of a fuel reformer and a fuel cell. A fuel reformer decomposes the fuel into hydrogen, carbon monoxide and carbon dioxide. In the category of portable miniature (and especially in man-wearable) RMFCs, PEM fuel cells have the widest use,

* Corresponding author. Tel.: +386 1 4773798; fax: +386 1 4773994.

E-mail address: gregor.dolanc@ijs.si (G. Dolanc).

mainly due to solid phase electrolyte and relatively low operating temperatures (50–80 °C for low temperature PEMFCs, and 100–200 °C for high temperature PEMFCs). Low temperature PEMFCs do not tolerate carbon oxide, so it must be removed. For this type of power source the efficiency and energy density are higher, but the overall system complexity increases. The fuel reformer is a complex unit composed of at least a reforming reactor, a combustor, an evaporator and possibly also a CO removal reactor. The most widely used process for producing hydrogen from methanol is steam reforming, with the highest yield of hydrogen obtained at nearly complete conversion at temperatures lower than 250 °C. A comprehensive setup of peripheral and control equipment is also needed to operate the system. The miniaturization of the reformer and its integration with the fuel cell has been a major research activity for the successful development of PEMFC-based systems over the last fifteen years.

In our work we focused on the design and implementation of a miniature reformer of methanol, aimed at feeding a low-temperature PEM fuel cell with electric power up to 100 W. Several prototypes of miniature scale reformers have been reported in the literature. For example in Refs. [3], [4] and [5] several prototypes of reforming reactors are presented, but they are not thermally self-sustained and they do not provide CO removal. In Refs. [6], [7] and [8] more complete and integrated prototypes are reported, containing also fuel evaporators and catalytic combustor, which means that they do not depend on external (electric) heating sources. Most of the presented systems are early prototypes demonstrated in a laboratory environment using laboratory peripheral and control equipment, such as laboratory pumps, stand-alone gas mass flow controllers (MFCs) or meters (MFMs). This kind of equipment cannot usually be embedded into a miniature system due to its size, price, power consumption, and many other parameters. Several miniature systems that aim at a higher technology level by being thermally self-sustained and in some cases also containing a CO removal reactor have been presented in the recent literature, a literature overview can be found in Refs. [9] and [10]. One such system is reported in Ref. [11] and is implemented as a single structure with a combustor, preheaters, a reformer reactor and a water gas shift reactor, but it does not include a final CO removal reactor. Similarly, in Ref. [12] a tubular quartz reactor structure composed of two concentric tubes is presented. Combustor, evaporator, reforming reactor and CO removal reactor (methanation) are all integrated into one quartz structure. The problem with the integration of the reforming reactor and CO removal reactor is that they require different operation temperatures, and this is difficult to achieve within a miniature and monolithic reactor structure. Operating at the same temperature may lead to non-optimal operation of one or both reactors. The system, presented in this paper, is designed to maintain the reformer and CO removal reactors at different temperatures, which leads to a more complex design, but makes it possible to achieve more optimal operation. In Ref. [13] another interesting integrated reactor concept is presented that is composed of a ceramic micro-channel monolith with several parallel channels, some employed for combustion and heating and some for reforming. Thanks to the mixed position of the combustion and reforming channels, good internal heat exchange and self-insulation is achieved. For the supply and distribution of reagents and the collection of products, relatively complex and precisely machined metal distributor elements and seals are required, which is somewhat similar to the approach used in our system. The system does not include a CO removal reactor and does not include evaporators, as the water/methanol mixture is evaporated and supplied to the reformer reactor by passing inert carrier gas through the bubbler, which is filled with a mixture of methanol and distilled water. The use of

additional inert gas may be acceptable for research but it is less convenient for final implementation. All three mentioned systems depend on laboratory equipment for the supply of input flows, measurements and control. In our case all the equipment (the manifold, pumps, tanks, sensors, electronic control unit and thermal insulation elements) is integrated into the system. In addition, our system was also designed for easy maintenance and servicing by providing the possibility of disassembling and replacing the main parts including the catalyst. This is usually not possible in the case of monolithic structure systems, as presented in the literature. Some similar systems are already available on the market, e.g. Refs. [14] and [15]. These are complete RMFC power sources, but they use high temperature PEM fuel cell, which means that CO removal reactor is not present in the system since this kind of fuel cell can tolerate higher concentration of CO (up to 1%).

Our goal was to design a complete reformer system reaching technology readiness level 6–7 [16], which represents a fully functional system prototype that has been demonstrated in an operational environment. This entails building the complete reformer system, including the peripheral and control equipment. The basic technologies of the reactor design and catalyst preparation and deposition are essential for the optimal operation of the system. This part of the design has been addressed in detail and was presented in our previous papers [17–21]. However, to upgrade the basic technologies and prototypes to operational systems, basic manufacturing and control technologies must be integrated and coordinated. This is particularly challenging in miniature scale systems.

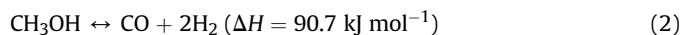
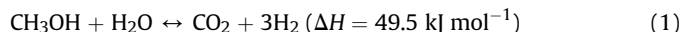
For optimal reactor operation, the relevant process parameters (the flow rates of the reactants, the temperatures of the reactor) must be controlled. The closed loop control concept is traditionally used to control process parameters, but this approach requires sensing, actuation, and control elements. While this can be readily applied in medium- and large-scale processes, there are limitations at miniature scale. The reason is that miniature sensors and actuators are not easily available and their use expands the setup and makes the miniature system more complex. To keep the system miniature and lightweight, all system components, including control elements, have to be optimised not only for performance, but also for small dimensions, lightweight and compact design, and it must be possible to elegantly integrate them into the process. One preferable option is the seamless integration of sensors with the process equipment [3], e.g. “printing” the sensors on the reactors.

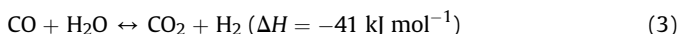
To achieve acceptable energy efficiency of the overall system, the internally consumed electric power should be far lower than the generated electric power. Therefore, it is necessary to minimise electricity consumption by designing reactors with a low pressure drop, by designing/selecting low power control and actuation elements, and minimising or even omitting the control elements by using passive techniques [22].

In the paper we summarise the system design, emphasising its miniaturisation, integration, process control, and raising the technology readiness level.

2. Background

In the presented system, conversion of methanol into hydrogen is performed by a steam reforming process. The output reformat gas, which is rich in hydrogen, can then be fed into a fuel cell and converted into electricity. The chemistry of steam reforming is well known and can be described by the following equations:





Reactions take place in the catalytic reactor, typically between 200 and 250 °C. Since the process is endothermic, it requires an external supply of thermal power, which should usually be generated by a combustor. For heat transfer, combustor and reforming reactors are joined over a common contact surface. The reformate gas at the output of the reformer typically contains up to 1% of CO, which can only be tolerated by high temperature PEM fuel cells. In the case of low temperature PEM fuel cells, the content of CO has to be removed (reduced). In general, this can be achieved by a cleaning catalytic reactors, where water gas shift (WGS) and preferential oxidation (PROX) reactions take place, which shift and oxidize the CO to CO₂, respectively. By using a new Cu_xCe_{1-x}O_{2-y} PROX catalyst [17], [18], the CO is oxidized by the addition of oxygen (air) with high selectivity (over 95%) at high conversion of CO (over 98%) at temperatures between 160 and 220 °C, leaving hydrogen unaffected:



This catalyst supports PROX reaction at CO concentrations in hydrogen rich reformate well above 2%. Thus, one can avoid the slowest processes among the hydrogen cleaning processes – high-temperature and low-temperature water gas shifts (HT and LT WGS).

3. System design

Fig. 1 shows the technological scheme of the system. The entire setup is divided into three subsystems: the actuator unit, the reactor unit and the control unit. The units are designed for their integration, but they can also be used separately.

3.1. The actuator unit

The actuator unit generates and controls the flow rates of methanol and water to the reforming reactor, air to the PROX reactor, and the air/methanol mixture to the catalytic combustor. The main design parameter is the maximum electric power of the power source, which is aimed at 100 W. To provide this electric power, the fuel cell must be supplied with 85 L h⁻¹ at 25 °C and

1 bar of hydrogen, as the efficiency of a typical 100 W PEM fuel cell is around 40%. This hydrogen production rate requires 50 mL h⁻¹ of methanol and 22 mL h⁻¹ of water to be fed into the reforming reactor. Usually a surplus of water (+30%, i.e. 29 mL h⁻¹) is required to avoid coke formation at the reforming catalyst.

For optimal process operation, the flow rates of methanol and water to the reactors must be kept close to the required values. Generally, input flow rates to the reactors are affected by the back pressure due to flow resistance and due to the volume increase during the chemical reaction. The control system must compensate for back pressure, e.g. by measuring the actual flow rate by the sensor and adjusting the flow actuator command accordingly. In our case, miniature pulse-operated metering pumps Pm and Pw (KNF FMM 20) are used for supply of methanol and water from storage tanks T2 and T3 to the reforming reactor. Thanks to the almost invariant relation between the pulse frequency and flow rate up to 1 bar of back pressure, flow sensors can be omitted. The control unit adjusts the flow rates simply by setting the pulse frequencies in the open loop. With each electric pulse, the pump pushes a predefined amount of liquid (pulse volume) towards the reactors. The pulse volume can be adjusted mechanically between 5 and 25 µl by adjusting the stroke of the pump. For both pumps, the pulse volume is adjusted to approximately 6.7 µl, so that at a pulse frequency of 5 Hz the flow rate is 120 mL h⁻¹. Pulse operated pumps also fulfil an additional technical demand, i.e. liquid tightness in both directions in a de-energised state, which prevents leakage from the tanks during power off.

For the supply of air to the PROX reactor, a miniature DC voltage diaphragm pump Pc is used. The air flow rate is adjusted by the DC voltage, considering the voltage/flow map. The required air flow rate for PROX is calculated as:

$$\phi_{A_PROX} = \phi_{H_2} x_{CO} (0.5/0.21) \quad (4/3) \quad (5)$$

ϕ_{A_PROX} – air flow rate to the PROX reactor (L min⁻¹ at 25 °C and 1 bar)

ϕ_{H_2} – hydrogen flow rate (1.42 L min⁻¹ = 85 L h⁻¹ at 25 °C and 1 bar)

x_{CO} – molar fraction of CO in reformate gas (approximately 1%)

0.5 – amount of O₂ needed for oxidation of 1 mol of CO

0.21 – molar fraction of oxygen in air

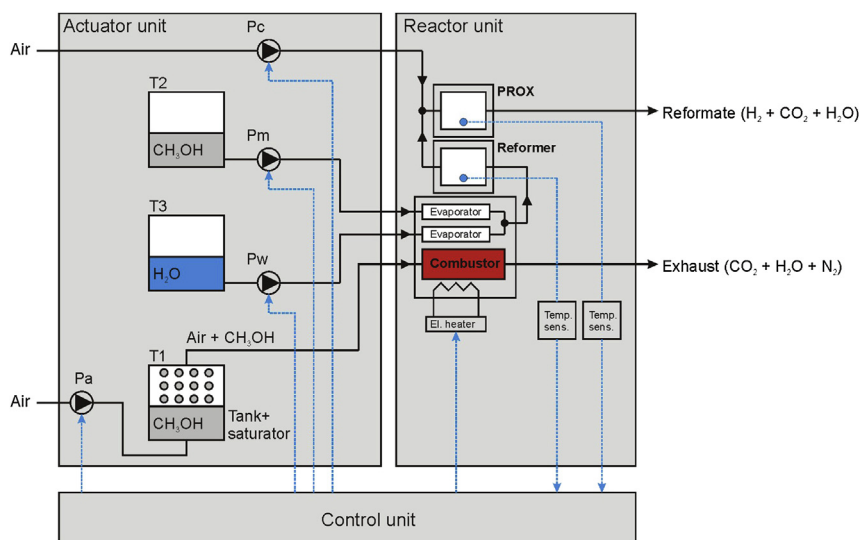


Fig. 1. Technological scheme.

4/3 – the ratio between the reformat and hydrogen flow rates, as follows from Eq. (1)

Assuming up to 1% CO concentration in the reformat, a suitable air flow rate to the PROX reactor (ϕ_{A_PROX}) is 0.05 L min^{-1} at 25°C and 1 bar.

The combustor must provide the thermal power for evaporation of methanol and water and heating them up to the reaction temperature 250°C , which requires 40 W of thermal power. In addition, thermal power of 6 W is needed to compensate for thermal losses due to the endothermic reforming reaction. Therefore, the theoretical required thermal power for the processing of 50 mL h^{-1} of methanol is 46 W, not including thermal losses to the environment. Based on temperature control experiments, we determined the combustor thermal power to be at least 100 W. Some extra power is needed to compensate for thermal losses to the environment and to reduce the warm-up period.

The combustor is fed by an air/methanol mixture, generated by the saturator. Air pump Pa (a DC voltage diaphragm pump KNF NMP 830 KNDC) generates the air flow, which is directed to the bottom of methanol tank T1, which acts as a methanol storage and saturator. When passing through the methanol, air is mixed with methanol vapour. The air/methanol mixture then leaves tank T1 and enters the catalytic combustor. As follows from Eq. (6), the oxygen/methanol molar ratio for the complete combustion should be 1.5 or higher:



Therefore, for 100 W of thermal power 20 mL h^{-1} of methanol and at least 80 L h^{-1} at 25°C and 1 bar of air must be fed into the combustor. By decreasing the air flow through the saturator, the residence time of air in the saturator increases and consequently the oxygen/methanol ratio decreases. At very low pump speed and consequently long residence time, the air/methanol mixture becomes saturated, containing 21.5% methanol and 78.5% air, at ambient temperature. In this case the oxygen/methanol ratio is 0.79, which is almost two times too low. To increase the ratio, the pump Pa air flow must be increased. It was determined experimentally that for the present saturator geometry, air flow must exceed 2 L min^{-1} at 25°C and 1 bar for the oxygen/methanol ratio to be above 1.5.

The mechanical design of the actuator unit and integration of the components is shown in Fig. 2. The main integration element is

the manifold, which is implemented by the two aluminium plates and the graphite seal in between (M7, M9, and M8). The manifold acts as a mounting support for the tanks, pumps, and reactor unit and it forms micro-channels to connect them. Thanks to the low volume of the channels, the priming time of the system is in the range of seconds. Tank element M1 is machined from one piece of polyoxymethylene (POM), which is resistant to methanol. The element has three cavities, forming tanks T1, T2, and T3, which are covered by plate M2 and three rubber seals M3. The air/methanol vapour mixture leaves the tank/saturator T1 at the top and it travels through the evaporator cover M4 and evaporator pipe M5 down to the manifold.

3.2. The reactor unit

The reactor unit is implemented as a metal/ceramic structure and includes a combustor with integrated methanol and water evaporators, a reforming reactor, and a PROX reactor. The cross-section of the structure and the elements are shown in Fig. 3 below:

A catalytic combustor with integrated evaporators is implemented as a stainless steel structure with top and bottom plates P1 and P3 and graphite seal P2 in between. Three cavities are machined in plate P3: the central cavity represents the combustor, while the left and right cavities represent the evaporators for water and methanol. The evaporator cavities are filled with ceramic fibre (not shown in the Figure) to increase flow resistance and minimise the evaporation pulsation. A metal mesh deposited by Pt is placed inside the central cavity, acting as a combustion catalyst. The sizes of cavities were determined by scaling the preceding experimental elements. The combustor is equipped with a 10 W electric pre-heater (A1), to ignite the combustion. The reforming and PROX reactors are implemented as ceramic (low temperature co-fired ceramics – LTCC) structures P5 and P9, both equipped with printed resistive PTC temperature sensors. Reforming reactor P5 is mounted on top of combustor plate P3. Thermal conductivity between the combustor and the reactor is increased by applying a thin film of a graphite thermal paste in between.

To simplify the system, there is only one temperature control loop, consisting of pump Pa and a temperature sensor to control the reformer reactor temperature. The PROX reactor temperature is also measured, but it is controlled indirectly by establishing a fixed temperature difference of approximately 80°C between the reforming and PROX reactors. The temperature difference is created

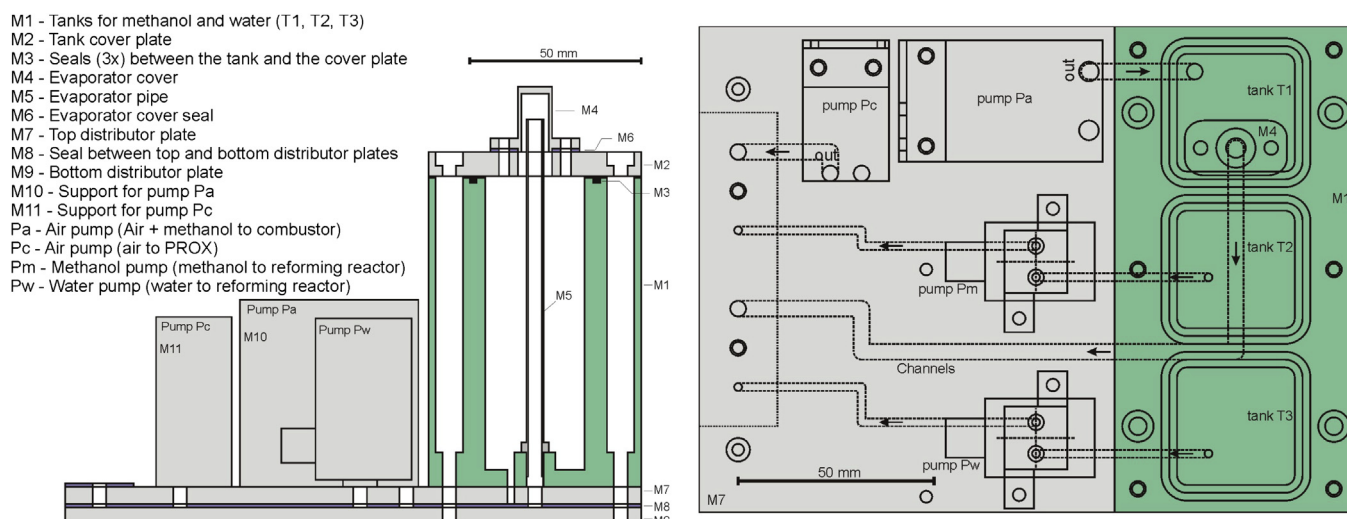


Fig. 2. The actuator unit (left: cross-section, right: top-down transparent view).

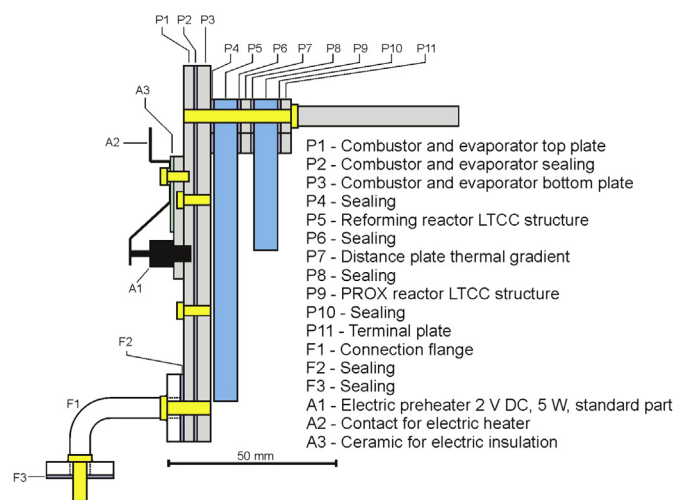
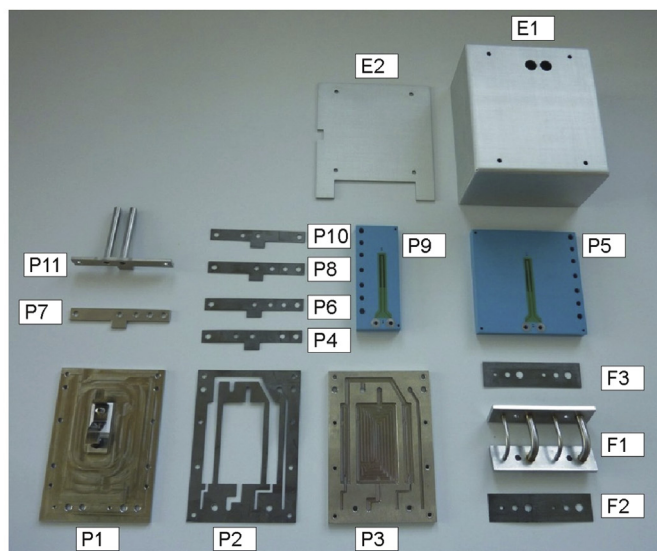


Fig. 3. The reactor unit (left: cross-section, right: elements).

by the air gap formed by distance plate P7 placed between the reactors. It was determined experimentally that a 2 mm gap creates the required temperature difference.

On top of distance plate P7, PROX reactor P9 is mounted and covered by terminal plate P11, which represents a binding flange for all the elements. By connecting the elements with two screws on one edge only, mechanical stress due to different thermal expansion of ceramic and metal is minimised. Two metal pipes are welded to terminal plate P11. The central pipe represents the exhaust from the catalytic combustor and the side pipe represents the exit of the reformat gas from the PROX reactor. Graphite seals P4, P6, P8, and P10 are used to ensure an elastic and gas-tight connection between the elements. In the connection area, the gas flow path between the combustor and the reactors is implemented. For thermal insulation and protection, structure P1–P11 is covered by an aluminium enclosure (E1 + E2). The empty space between the enclosure and the structure is filled with insulation material (ceramic fibre). The reactor unit is connected to the actuator unit by the 4-channel flange F1 and graphite seals F2, F3. The flange is designed to minimise the heat transfer from the reactor unit to the actuator unit in order to keep the actuator unit cool.

Generally, in micro-reactors, the catalyst can be deposited directly on the internal surface, which is maximised by micro-channel design, as in e.g. Refs. [3] and [4]. The other method involves using monoliths made of porous metal or ceramic and integrated into the reactor, as can be seen in Ref. [6] or [8]. In our case, the reforming and PROX reactors are designed to be filled with catalyst particles or coated beads (ceramic spheres), the same principle can also be found in Refs. [23] and [24]. We found this option attractive due to the possibility to maintain and replace the catalyst during the entire life-cycle of the device. Therefore, the reactors (P5, P9) are implemented as ceramic structures with internal cavities. Both reactors are implemented by means of LTCC technology, as described in Refs. [20] and [21]. This is a very attractive technology for micro-reactor design since 3D structures with cavities and micro-channels can be manufactured, offering sufficient mechanical strength, chemical inertness, and the possibility of elegant integration of sensors (temperature, pressure). The reactor geometry was designed by computational fluid dynamic modelling and confirmed with prototype reactors. Both reactors



have a similar structure, but different sizes, since the reforming process requires a significantly greater catalyst volume than PROX. The volumes of the reforming and PROX reactor cavities are 18.7 cm³ and 5.4 cm³, respectively. Fig. 4 shows the appearance of the reactors and internal structure of the reformer reactor after cross cutting. Each reactor is built from 46 layers, which were laser cut from green (raw) LTCC tapes, laminated together, and then fired at a temperature of 850 °C. To prevent the catalyst particles or beads from escaping from the reactor, there are inlet and outlet grids, consisting of a number of small holes (1.2 × 0.3 mm²). A service port is provided to put in or replace the catalyst.

Thanks to the combustor design and high thermal inertia of its metal structure, a very uniform temperature profile across the reactor is achieved. Study [23] confirmed experimentally that even temperature distribution is an important factor for optimal reforming and low CO concentration.

For reforming, HiFUEL R120 industrial catalyst (CuO/ZnO/Al₂O₃) from Alfa Aesar was used. The BET specific surface area was measured to be 81.5 m² g⁻¹. The reactor was filled with 4.3 g of the 400–500 μm sieved fraction. The activity of the catalyst was first tested in the experimental reactor. At a reaction temperature of 250 °C and steam to methanol ratio of 1.3, 100% methanol conversion was achieved at a methanol flow rate of 50 mL h⁻¹. The composition of the gaseous mixture at the exit of the reactor was as follows: $x_{\text{CO}} = 0.2$ mol%, $x_{\text{CO}_2} = 6.5$ mol%, $x_{\text{H}_2\text{O}} = 40.7$ mol% and $x_{\text{H}_2} = 52.6$ mol%.

For the PROX, a Cu_xCe_{1-x}O_{2-y} nanostructured catalyst can be used. This catalyst was developed at the National Institute of Chemistry, applied for a patent and described in several publications [17], [18]. The catalyst is capable of oxidizing CO in the presence of excess H₂ with a stoichiometric flow of O₂ at a selectivity over 95% and conversion over 98% between 160 °C and 220 °C.

3.3. The control unit

An electronic control unit (ECU) was designed to closely meet the demands of the system. The number and types of I/O signals are tailored to the sensors and actuators to connect them directly without any additional interfaces. Programming and data logging is performed over a personal computer. The block diagram of the control unit is shown in Fig. 5, left.

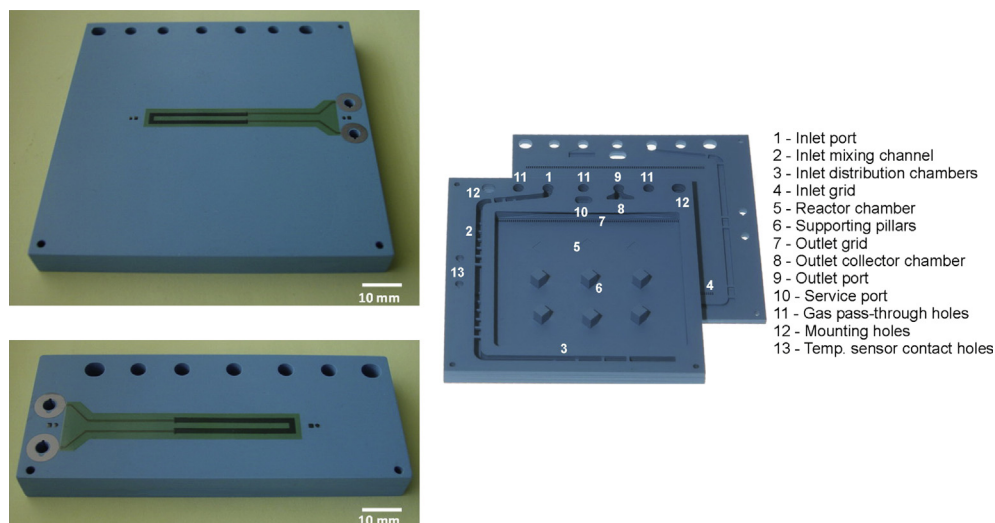


Fig. 4. LTCC structures (left top: reformer reactor; left bottom: PROX reactor; right: reformer reactor cross-section).

The control program is implemented in terms of a finite state machine with the state transition diagram shown in Fig. 5, right top. After power on, the system idles in state S1-Stopped, all actuators are de-energised. When the user triggers the “Start” command, the system enters the state S2-Ignition. In the case of a cold start (with reformer reactor temperature below 70 °C), the combustor is first preheated by an electric heater for a fixed period of time. Then saturator pump Pa is activated at 50% of full speed. When the reformer temperature reaches 100 °C, ignition is considered successful. After the ignition, the transition to the S3-PreheatingA state is performed, which is used for heating the reactors by convection. When the temperature reaches 170 °C and 130 °C in the reforming and PROX reactors, respectively, the system enters the S4-PreheatingB state, which is used for further heating of the reactors by convection and steam. After reaching the target

temperatures, the system enters the final S5-Operation state, where hydrogen production is performed. In this state, the methanol and water flow rates to the reformer reactor and air flow rate to the PROX reactor are controlled automatically according to the required hydrogen production rate. At any time the user can trigger the “Stop” command, resulting in a transition to the S1-Stopped state.

In states S3, S4, and S5 the reformer reactor temperature control is activated. It is implemented as a simple two-state on/off control (Fig. 5, right bottom). Based on the deviation between the required (T_{set}) and actual temperature (T) of the reforming reactor, and the deadband D (1.5 °C), the combustor power is switched on and off by setting the air pump (Pa) speed between nominal and zero speed. In general, this kind of control results in the oscillation of the process variable around the setpoint. But due to the high thermal

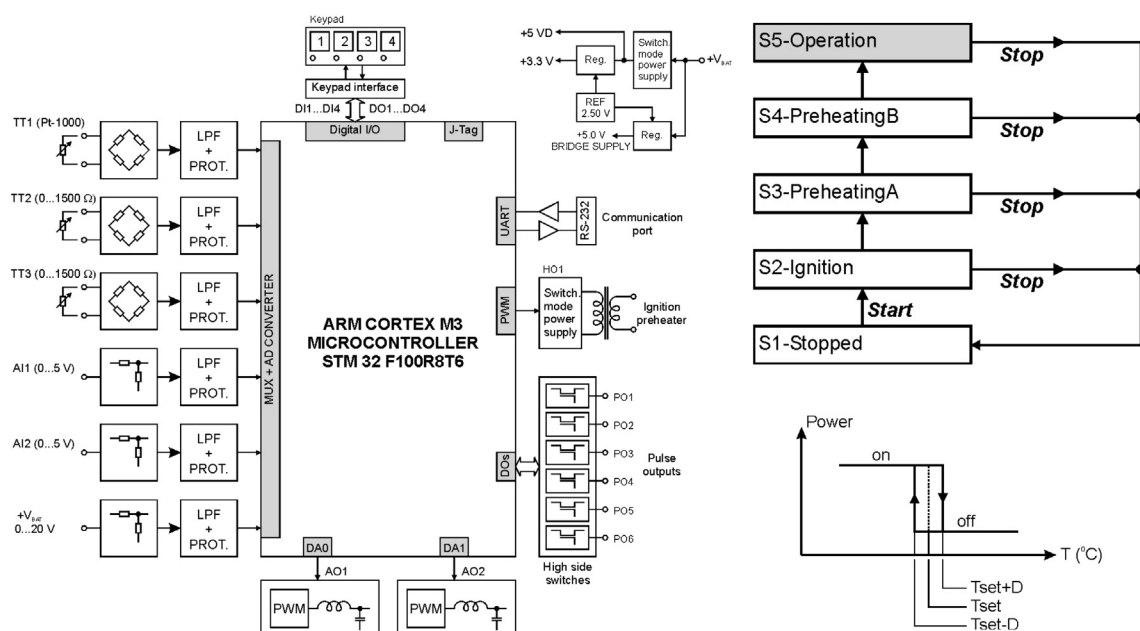


Fig. 5. The control unit (left: block diagram; right top: state machine; right bottom: temperature control).

inertia of the combustor and reactor structures and the low order dynamic of the heating process, temperature oscillations can be made relatively low. The other possible solution would be continuous control, as in e.g. Ref. [25] or [26], but a prerequisite for this approach is the ability to maintain the correct oxygen/fuel ratio over the entire power range, which is not possible with the present saturator concept.

The user interacts with the system over a keypad with LED indicators. The currently active state and error code are indicated by a blinking pattern of LE diodes.

4. Results and discussion

Fig. 6 shows the complete system with the reactor unit, actuator unit, and control unit integrated. Particular functions of the system were evaluated experimentally.

4.1. Reforming

Reforming efficiency was tested in a laboratory for several days, 8 h per day at a nominal operating point (methanol flow rate 50 mL h⁻¹, water flow rate 29 mL h⁻¹, reformer reactor temperature 250 °C). Reformate quality was evaluated by gas chromatography (Agilent 7890A). The composition of the reformate gas is given in Table 1. Note that during the test, the PROX reactor was inactive and filled with inert ceramic spheres.

4.2. Saturator operation

The actual oxygen/methanol ratio of the mixture generated by the saturator was estimated. The oxygen flow rate ϕ_{O_2} (mol min⁻¹) was estimated from the air flow rate of pump Pa:

$$\phi_{O_2}(\text{mol min}^{-1}) = 0.21\phi_A(\text{L min}^{-1}) / 24.8 \text{ L mol}^{-1} \quad (7)$$

0.21 – molar fraction of oxygen in air

ϕ_A – volumetric air flow rate generated by pump Pa (L min⁻¹ at 25 °C and 1 bar)

24.8 – molar volume (L mol⁻¹) of ideal gas at 25 °C

Table 1

Gas chromatographic analysis of the reformate (molar fraction %).

CO ₂	H ₂ O	CH ₃ OH	H ₂	CH ₄	CO
21.561	10.331	2.210	65.292	0.200	0.406

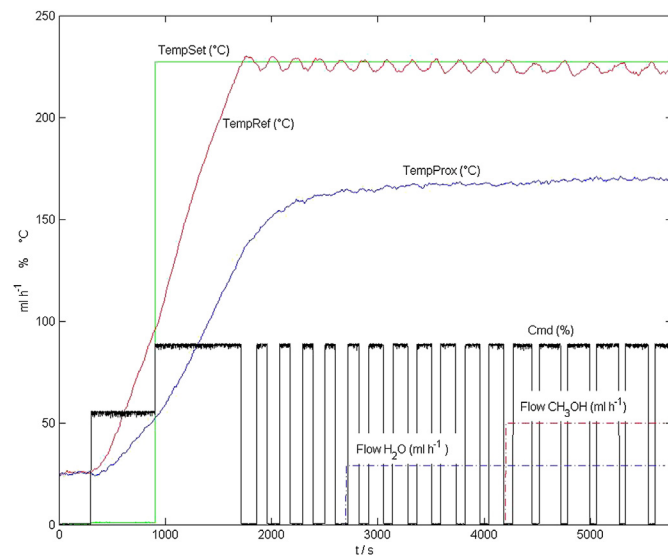


Fig. 7. Temperature control.

The methanol flow rate ϕ_{CH_3OH} (mol min⁻¹) was estimated simply from the methanol level drop in tank T1 after operation period t at constant pump speed:

$$\phi_{CH_3OH}(\text{mol min}^{-1}) = A(\text{cm}^2) \cdot \Delta h(\text{cm}) \rho(\text{g cm}^{-3}) / M(\text{g mol}^{-1}) / t(\text{min}) \quad (8)$$

A – area of the tank T1 (16 cm²)

Δh – drop of the methanol level (cm) in tank T1 in time t

ρ – methanol specific weight (0.7918 g cm⁻³)

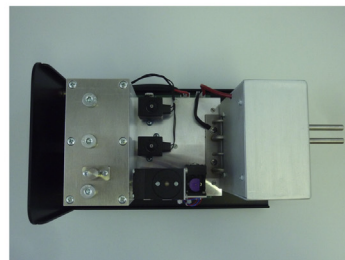
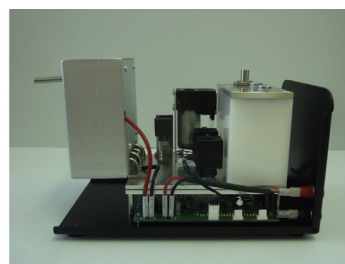
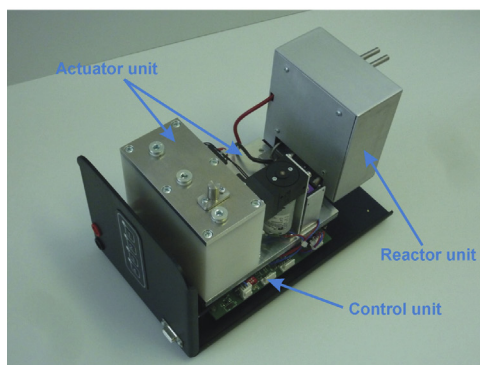


Fig. 6. Integrated system.

Table 2
Thermal power of the combustor.

Period	Thermal power utilisation	Ton	Toff	Duty cycle	Power measured	Power increase measured	Power increase theoretical
1	- Thermal losses	97 s	115 s	45.8%	72.3 W	—	—
2	- Thermal losses	141 s	87 s	61.8%	99.7 W	+27.4 W	+22.9 W
3	- Evaporation H ₂ O, 29 mL h ⁻¹						
	- Thermal losses	212 s	61 s	77.7%	122.7 W	+23 W	+22.8 W
	- Evaporation H ₂ O, 29 mL h ⁻¹						
	- Evaporation CH ₃ OH, 50 mL h ⁻¹						
	- Reforming CH ₃ OH, 50 mL h ⁻¹						

M – methanol molar mass (32.04 g mol⁻¹)
 t – operation duration (min)

The oxygen and methanol flow rates, oxygen/methanol ratio (ϕ_{O_2}/ϕ_{CH_3OH}), and thermal power were estimated at a nominal air flow rate of $\phi_A = 2.7$ L min⁻¹ at 25 °C and 1 bar. The methanol flow rate was 0.013 mol min⁻¹, the thermal power was 158 W, and the ratio was 1.76, enabling complete combustion. At reduced flow rate, e.g. at $\phi_A = 1$ L min⁻¹ at 25 °C and 1 bar, the ratio decreased to 1.14, which leads to incomplete combustion.

4.3. Temperature control

Fig. 7 shows the temperature time profiles during operation. The reforming reactor temperature ($Temp_{Ref}$) oscillates slightly around the setpoint ($Temp_{Set} = 235$ °C), which is a consequence of the on/off control principle. An oscillation range of 5 °C is believed to not have any negative influence on reformer reactor operation. The PROX reactor temperature ($Temp_{Prox}$) is very stable and inside the required temperature window (160–220 °C), which confirms the effect of the air gap.

4.4. Combustor operation

The actual thermal power of the combustor was estimated by multiplication of the nominal (i.e. maximum) power at uninterrupted operation (158 W) and the duty cycle (%) of the temperature controller (signal Cmd in Fig. 7). The duty cycle was calculated from the durations of the “on” and “off” intervals of combustor operation. In the first period (2000–2700 s), reforming and evaporation were not active. The thermal power was 72 W and utilised for compensation of the thermal losses. In the second period (2700–4200 s), 29 mL h⁻¹ of water was fed into the reactors. Thermal power increased to 99.7 W due to evaporation and heating of the water from 25 °C to 235 °C. In the third period (4200–5700 s), in addition to 29 mL h⁻¹ of water, also 50 mL h⁻¹ of methanol was fed into the reactors. The thermal power of the combustor increased to 122.7 W due to methanol heating, evaporation, and reforming. Estimated power increase steps agree very well with the theoretical values, as follows from the last two columns in Table 2 below.

4.5. Energy efficiency and specific energy

The energy efficiency of the reformer system was calculated by relation Eq. (9). During steady operation, 50 mL h⁻¹ of methanol is consumed for the reforming, plus 24.7 mL h⁻¹ for heating power of 122.7 W. This results in a total methanol flow rate of 74.7 mL h⁻¹, which corresponds to an input thermal power of $P_{th,in} = 372$ W. The generated hydrogen flow rate of 83 L h⁻¹ corresponds to an output thermal power of $P_{th,out} = 252$ W.

$$\eta_{REF} = P_{th,out}/P_{th,in} = 252 \text{ W}/372 \text{ W} \approx 67.7\% \quad (9)$$

The energy efficiency of the reformer could be increased by decreasing thermal losses, but this would require more insulation, leading to an increased physical size of the system.

The energy efficiency of the electric power source can be estimated by relation Eq. (10). The efficiency of small low-temperature PEM fuel cells is around 40%, which means that a hydrogen flow of 83 L h⁻¹ is converted to electric power $P_{el} = 100$ W. However, a small part of the electric power $P_i = 3$ W is consumed internally by the control and actuation elements of the reformer and fuel cell. As a result, a power source efficiency of 26% can be expected, as follows from relation Eq. (10):

$$\eta_{PS} = (P_{el} - P_i)/P_{th,in} = (100 \text{ W} - 3 \text{ W})/372 \text{ W} \approx 26\% \quad (10)$$

One interesting parameter is the specific energy of the power source (Wh kg⁻¹), which specifies the amount of stored energy per mass. In the case of fuel cell power sources, the specific energy increases asymptotically with the mass of the stored fuel. If we require operation time $t_{op} = 24$ h, then the masses of the stored fuel (m_{CH_3OH}) and water (m_{H_2O}) are 1.420 kg and 0.696 kg, respectively. In addition, the mass of the complete reformer system (m_{REF}) is 3 kg and the mass of a typical 100 W low-temperature PEM fuel cell (m_{FC}) is assumed to be around 1.3 kg. The specific energy can then be calculated as:

$$E_{sp} = P_{el} t_{op}/(m_{CH_3OH} + m_{H_2O} + m_{REF} + m_{FC}) = 374 \text{ Wh kg}^{-1} \quad (11)$$

The specific energy could be increased by reducing the mass of the system, by improving the efficiency of the small size fuel cells, and also by increasing the thermal efficiency η_{REF} of the reformer system.

5. Conclusion

In this work, a miniature methanol reformer was engineered as a hydrogen source for fuel cell power source. The goal was to exceed the laboratory level by building a complete system consisting of reactors, a combustor, an evaporator, and control elements. The engineering aspects of the design, integration, and fabrication of the elements in miniature scale were addressed. After the fabrication and assembly, the system was tested in a laboratory environment; control functions, reformat quality, and energy efficiency were analysed.

6. Disclaimer

The views expressed in this paper can in no manner be taken to reflect the official opinion of the European Space Agency.

Acknowledgements

This work was funded by the Government of Slovenia through a European Space Agency (ESA) contract (No 4000103742/11/NL/KML) under PECS (Plan for European Cooperating States).



References

- [1] S. Mekhilef, R. Saidur, A. Safari, *Renew. Sust. Energy Rev.* 16 (2012) 981–989.
- [2] <http://www.sfc.com/en>.
- [3] Y. Kawamura, N. Ogura, T. Yamamoto, A. Igarashi, *Chem. Eng. Sci.* 61 (2006) 1092–1101.
- [4] G. Park, D.J. Seo, S. Park, Y. Yoon, C. Kim, W. Yoon, *Chem. Eng. J.* 101 (2004) 87–92.
- [5] K.R. Hwang, C.B. Lee, S.K. Ryi, S.W. Lee, J.S. Park, *Int. J. Hydrogen Energy* 37 (2012) 6601–6607.
- [6] J.D. Holladay, E.O. Jones, M. Phelps, J. Hu, *J. Power Sources* 108 (2002) 21–27.
- [7] E. Calò, A. Giannini, G. Monteleone, *Int. J. Hydrogen Energy* 35 (2010) 9828–9835.
- [8] T. Kim, *Int. J. Hydrogen Energy* 34 (2009) 6790–6798.
- [9] J.D. Holladay, Y. Wang, E. Jones, *Chem. Rev.* 104 (2004) 4767–4790.
- [10] A. Iulianelli, P. Ribeirinha, A. Mendes, A. Basile, *Renew. Sust. Energy Rev.* (2014) 355–368.
- [11] L. Pan, C. Ni, X. Zhang, Z. Yuan, C. Zhang, S. Wang, *Int. J. Hydrogen Energy* 36 (2011) 319–325.
- [12] R. Chein, Y.C. Chen, J.Y. Chen, J.N. Chung, *Int. J. Hydrogen Energy* 37 (2012) 6562–6571.
- [13] A.M. Moreno, B.A. Wilhite, *J. Power Sources* 195 (2010) 1964–1970.
- [14] <http://www.ultracell-llc.com>.
- [15] <http://serenergy.com/products/systems/h3-350/>.
- [16] Technology Readiness Levels Handbook for Space Applications, ESA, September 2008. TEC-SHS/5551/MG/ap, Issue 1, Revision 6.
- [17] G. Avgouropoulos, T. Ioannides, H. Matralis, J. Batista, S. Hočevár, *Catal. Lett.* 73 (2001) 33–40.
- [18] G. Avgouropoulos, T. Ioannides, Ch. Papadopoulou, J. Batista, S. Hočevár, H. Matralis, *Catal. Today* 75 (2002) 157–167.
- [19] A. Pohar, D. Belavič, G. Dolanc, S. Hočevár, *J. Power Sources* 256 (2014) 80–87.
- [20] D. Belavič, M. Hrovat, G. Dolanc, M. Santo–Zarnik, J. Holc, K. Makarovič, *Radioengineering* 21 (2012) 195–200.
- [21] M. Hrovat, D. Belavič, G. Dolanc, P. Fajdiga, M. Santo–Zarnik, J. Holc, M. Jerlah, K. Makarovič, S. Hočevár, I. Stegel, *Inf. MIDEA* 41 (2011) 171–178.
- [22] K.F. Lo, S.C. Wong, *Int. J. Hydrogen Energy* 36 (2011) 7500–7504.
- [23] Harvey H.F. Wang, S.C. Chen, S.Y. Yang, G.T. Yeh, M.H. Rei, *Int. J. Hydrogen Energy* 37 (2012) 7487–7496.
- [24] C. Pan, R. He, Q. Li, J.O. Jensen, N.J. Bjerrum, H.A. Hjulmand, A.B. Jensen, *J. Power Sources* 145 (2005) 392–398.
- [25] S.J. Andreasen, S.K. Kær, S. Sahlin, *Int. J. Hydrogen Energy* 38 (2013) 1676–1684.
- [26] J. Jiang, X. Li, Z. Deng, J. Yang, Y. Zhang, J. Li, *Int. J. Hydrogen Energy* 37 (2012) 12317–12331.